Sivakumar, V. *et al.* (2010). *Géotechnique* **60**, No. 8, 595–609 [**doi:** 10.1680/geot.8.P.008]

Mechanical behaviour of unsaturated kaolin (with isotropic and anisotropic stress history). Part 2: performance under shear loading

V. SIVAKUMAR*, R. SIVAKUMAR†, J. BOYD‡ and P. MACKINNON*

Validation of a framework for unsaturated soil behaviour has frequently resulted in disagreement with basic propositions. A primary reason for this disparity is considered to be attributable to the anisotropic properties of the soil specimens tested as a result of preparation using one-dimensional compaction. As part of the work presented, comparison is made between tests on samples of unsaturated kaolin prepared at identical specific volumes and specific water volumes using isotropic compression and one-dimensional compression. The suctions in the samples were reduced to predefined values by wetting under low isotropic loading in a triaxial cell. The samples were then taken through various stress paths to failure, defined as the critical state strength, while the suctions were held constant. Stress path tests were also performed on samples without reducing the suction to predefined values. In the latter, constant water mass tests, the suctions were allowed to vary and were measured using a psychrometer. The results of the tests at critical state are compared with the propositions of Wheeler and Sivakumar. The shear strengths of samples with isotropic previous history are shown to be significantly greater than those of samples with one-dimensional stress history when plotted against the mean net stress. The normal compression lines, critical state lines and yield characteristics are also shown to be significantly influenced by the previous stress history and are shown to be different for isotropically and one-dimensionally prepared samples.

KEYWORDS: compaction; shear strength; stress path; suction; unsaturation

La validation d'un cadre pour le comportement des sols non saturés a donné lieu fréquemment à un désaccord relativement aux propositions de base. Une des principales raisons de cette disparité est généralement attribuée aux propriétés anisotropes des spécimens de sol testés à la suite d'une préparation effectuée par compactage unidimensionnel. Dans le cadre des travaux présentés, on effectue une comparaison entre les tests sur des échantillons de kaolin non saturé, préparés avec des volumes massiques identiques et des volumes d'eau spécifiques, en utilisant une compression isotrope et une compression unidimensionnelle. On réduit les aspirations dans les échantillons à des valeurs prédéfinies par mouillage sous faible charge isotrope dans un cellule triaxiale. On soumet ensuite les échantillons à différents types de contraintes jusqu'à la rupture, définies comme résistance à l'état critique, tout en maintenant les aspirations à des niveaux constants. On procède également à des tests sous contrainte sur des échantillons sans réduction de l'aspiration à des valeurs prédéfinies. Dans ces derniers tests à masse d'eau constante, on laisse varier les aspirations, que l'on mesure à l'aide d'un psychomètre. On compare les résultats des tests à l'état critique avec les thèses de Wheeler et Sivakumar (1995). Les résistances au cisaillement d'échantillons faisant l'objet de facteurs isotropes précédents s'avèrent sensiblement plus élevées que celles des échantillons caractérisés par une contrainte unidimensionnelle, lorsqu'on effectue les tracés en fonction des contraintes nettes moyennes. En outre, on relève que les contraintes survenues précédemment influent de façon significative sur les lignes de compression, les lignes à l'état critique et les caractéristiques de fléchissement normales, et s'avèrent être différentes pour les échantillons préparés de façon isotrope et unidimensionnelle.

INTRODUCTION

Several attempts have been made to extend the behavioural framework developed for saturated soil to unsaturated soil (Alonso *et al.*, 1987, 1990; Toll, 1990; Maâtouk *et al.*, 1995; Wheeler & Sivakumar, 1995; Blatz & Graham, 2003; Chiu & Ng, 2003). The frameworks for unsaturated soils vary in detail, but are essentially based on a similar principle that the mechanical behaviour can be separated into elastic and plastic components.

Alonso *et al.* (1987) were among the first researchers to suggest the concept of yielding in unsaturated soils in terms of suction, s, and mean net stress, $\overline{p}$, and postulated the existence of a yield locus, referred to as the loading–collapse (LC) yield locus, in the $\overline{p}$:s plane. Alonso *et al.* (1990) subsequently introduced a deviator stress component, q, into the model and proposed a yield surface in $\overline{p}$:q:s space. The yield surface can be viewed as a family of elliptical yield loci in constant suction planes as shown in Fig. 1(a). Cui & Delage (1996) examined the yield loci in the q: $\overline{p}$ plane by conducting stress probe tests and concluded that hardening effects on the shape of the yield locus were similar to those for saturated natural soils and resulted in a yield locus which is near-elliptical and inclined approximately along the K_0 axis (Fig. 1(b)), where K_0 is the coefficient of earth pressure at rest. Leroueil *et al.* (1985) and Cui & Delage (1996) attributed the inclination of the yield locus to the anisotropic nature of the unsaturated compacted soil tested. A material in which the stress–strain properties depend on the orientation of the sample is said to be 'anisotropic' (Graham & Houlsby, 1983) and anisotropy is recognised as an important feature in describing the behaviour of natural soils (Leroueil & Vaughan, 1990; Lings *et al.*, 2000).

Sivakumar & Wheeler (2000) suggested that one-dimensional compaction inevitably generates a degree of anisotropy in a soil (stress-induced anisotropy) and con-

Manuscript received 21 January 2008; revised 15 June 2009. Published online ahead of print 12 March 2010.
Discussion on this paper closes on 1 January 2011, for further details see p. ii.

* School of Planning, Architecture and Civil Engineering, Queen's University Belfast, UK.
† Atkins, Epsom, UK.
‡ University of Ulster, UK.

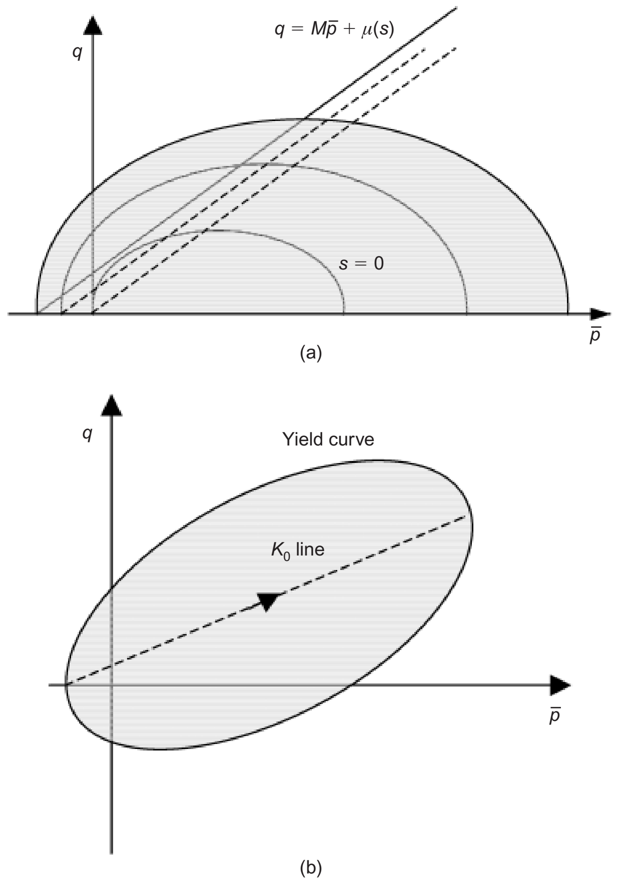

Fig. 1. Effects of anisotropy on the shape of the yield loci: (a) yield loci (Alonso *et al.*, 1990); (b) inclined yield locus for anisotropic compacted clays (Cui & Delage, 1996)

cluded that it adds complexity to the modelling of unsaturated soils. Accordingly, data obtained from samples with isotropic stress–strain properties would be desirable to obviate the complexity of constitutive modelling. However, most, if not all, published research on unsaturated soils has been carried out on samples with inherited anisotropy. As part of the research presented here, samples with initial isotropic stress–strain properties have been tested to critical state. The accompanying paper (Sivakumar *et al.*, 2010) deals in detail with the preparation and performance of such soils under isotropic loading and compares the findings with tests on initially one-dimensionally compressed samples. The work presented in this paper extends the work to shear loading and the validity of critical state concepts, and assesses the effects of anisotropy on the behaviour of unsaturated soils.

EXPERIMENTAL WORK

Part 1 of this study (Sivakumar *et al.*, 2010) describes the sample preparation techniques. In summary, samples of kaolin were prepared using two different procedures: isotropic compression and one-dimensional compression. The samples were prepared at 25% water content and at an initial specific volume of 2·19. Samples prepared isotropically are referred to as samples IS(A). The samples prepared by one-dimensional static compression are referred to as samples ID(A).

A number of samples of IS(A) and ID(A) were subject to reduction in suction to predefined values before being taken through various stress paths including isotropic compression and shear loading. The accompanying paper (Sivakumar *et al.*, 2010) discusses the findings from the isotropic compression testing while this paper deals with the findings from the shear loading phase of the testing. Tables 1 and 2 in the companion paper list the initial conditions of samples tested in IS(A) and ID(A). During the shear loading, most of the samples were taken through two different stress paths in the q: $\overline{p}$ plane, namely fully drained and constant $\overline{p}$ tests. However, a single test was conducted using a curved stress path (varying slope of $\mathrm{d}q/\mathrm{d}\overline{p}$ at a suction value of 200 kPa). The foregoing tests were performed under constant suction conditions using the axis translation technique. The results of a number of constant water mass tests on samples of IS(A) and ID(A) are also reported. In these tests the suctions were allowed to vary and were measured using a thermocouple psychrometer.

RESULTS AND DISCUSSION

The results of the testing are discussed under four specific headings.

(*a*) Critical state of the soil with isotropic stress history.
(*b*) Yield surface in q:$\overline{p}$:s space for samples with isotropic stress history.
(*c*) Effects of stress-induced anisotropy on the critical state and yield characteristics under controlled suction.
(*d*) Effects of stress-induced anisotropy on the stress–strain behaviour and stress paths of samples tested under constant water mass conditions.

Critical state of the soil with isotropic stress history

Figure 2 shows typical plots of deviator stress against axial strain for two samples with identical initial specific volumes and specific water volumes. The samples were tested under fully drained conditions after isotropic consolidation at a mean net stress of 150 kPa and suction of 100 kPa. The samples were sheared at a strain rate of 0·07%/h. This rate was established based on the coefficient of consolidation with respect to water volume change during the initial equalisation stage. Typically, fully drained shearing lasted about 4 weeks. The shearing was terminated on reaching the critical state, based on steady conditions being reached in specific volume v, deviator stress q, and mean net stress $\overline{p}$. The two stress–strain curves are essentially identical and the variation in deviator stress at failure is ±1·5%. The plots exemplify the quality of the experimental data reported.

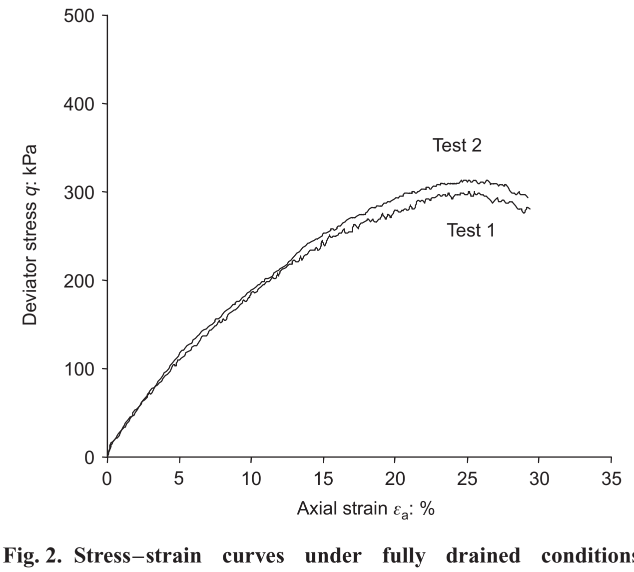

Fig. 2. Stress–strain curves under fully drained conditions (IS(A), suction of 100 kPa and mean net stress of 150 kPa)

A number of stress path tests were performed on isotropically prepared samples under controlled suction values of zero, 100 kPa, 200 kPa and 300 kPa. The stress path tests performed at 200 kPa of suction are shown in Fig. 3. Table 1 lists the conditions of the sample at the end of normal compression and critical state. The types of stress paths were fully drained, constant $\overline{p}$ and a curved path with varying slope. In all three cases, the sample volume reduced on shearing to the critical state. The data shown in Fig. 3, and similar plots for different suctions, confirm the existence of a unique critical state relationship with respect to q: $\overline{p}$ and v: $\overline{p}$. The conditions of the soil samples at the critical state in terms of deviator stress q, mean net stress $\overline{p}$, specific volume v and specific water volume v_w at different values of suction s are shown in Fig. 4. The linear equations suggested by Wheeler & Sivakumar (1995) and listed as equations (1) to (3) below may be used to define the relationships

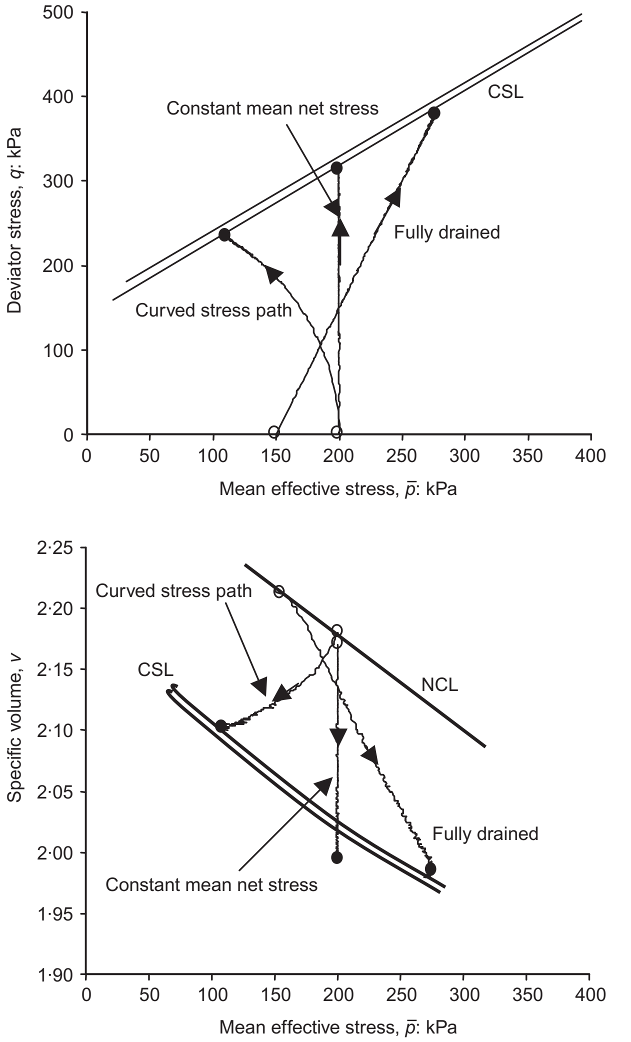

Fig. 3. Conditions at critical state at suction of 200 kPa for IS(A)

$$q = M(s)\overline{p} + \mu(s) \quad (1)$$

$$v = \Gamma(s) - \psi(s)\ln(\overline{p}/p_{atm}) \quad (2)$$

$$v_w = A(s) - B(s)\ln(\overline{p}/p_{atm}) \quad (3)$$

where the parameters $M(s)$, $\mu(s)$, $\psi(s)$, $\Gamma(s)$, $B(s)$ and $A(s)$ are the slopes and the intercepts of the critical state lines in the q: $\overline{p}$, v:ln ($\overline{p}$) and v_w:ln ($\overline{p}$) planes respectively. Early work in unsaturated soil (Bishop & Blight, 1963) considered the degree of saturation S_r as one of the controlling parameters and a similar approach has been used within the context of modern unsaturated soil mechanics by Toll (1990). Recent research work in unsaturated soils gives renewed interest in the use of S_r in the modelling of unsaturated soils (Gallipoli *et al.*, 2003; Wheeler *et al.*, 2003). However the authors limit the analysis of data within the context of two stress state variables.

Linear regression was used to evaluate the relevant parameters. The slopes of the critical state lines $M(s)$ in the q: $\overline{p}$ plane are 0.89, 0·93, 0·91 and 1·24 for suctions of zero, 100, 200 and 300 kPa respectively. The variation of the slope with suction is shown in Fig. 5(a). The effect of suction on the slope is relatively small up to 200 kPa of suction, although a significant increase in the value of the slope is observed at a suction value of 300 kPa, which contradicts the generally accepted view that $M(s)$ is constant with suction (Alonso *et al.*, 1990; Ng & Chiu, 2001; Wang *et al.*, 2002).

The intercepts of the critical state lines $\mu(s)$ are 0, 67 kPa, 130 kPa and 94 kPa for suction values of 0, 100, 200 and 300 kPa respectively. The relationship between $\mu(s)$ and suction is also shown Fig. 5(a). The variation of $\mu(s)$ is reasonably linear up to a suction value of 200 kPa. However, the intercept value drops significantly for the suction of 300 kPa. An increase in $\mu(s)$ with suction is reported elsewhere (Alonso *et al.*, 1990; Maâtouk *et al.*, 1995; Wheeler & Sivakumar, 1995; Futai & Almeida, 2005), but it is not unusual for the intercept to exhibit a reduction as shown, although the reason for this is unclear.

Table 1. Normally consolidated and critical state parameters (samples of IS(A))

Test no.	After isotropic compression				Critical state				
	$\overline{p}$: kPa	s: kPa	v	v_w	$\overline{p}$: kPa	s: kPa	q: kPa	v	v_w
1A (CP)	50	0	2·268	2·268	50	0	36	2·184	2·225
1B (CP)	100	0	2·146	2·146	100	0	79	2·080	2·139
1C (FD)	150	0	2·073	2·073	230	0	211	1·973	2·061
2A (CP)	100	100	2·196	1·917	100	100	160	2·054	1·924
2B (FD)	150	100	2·187	1·953	254	100	312	1·977	1·926
2B (FD)	150	100	2·161	1·927	250	100	300	1·983	1·916
2C (CP)	200	100	2·104	1·906	200	100	251	1·985	1·907
3A (CP)	200	200	2·171	1·832	200	200	318	1·995	1·863
3B (FD)	150	200	2·216	1·842	276	200	379	1·984	1·868
3C (SP)	150	200	2·180	1·843	108	200	234	2·101	1·883
4A (CP)	100	300	2·230	1·759	100	300	220	2·191	1·796
4B (FD)	100	300	2·233	1·761	222	300	368	2·011	1·810
4C (FD)	150	300	2·211	1·764	315	300	495	1·969	1·803

(CP), constant mean net stress; (FD), fully drained; (SP), stress path

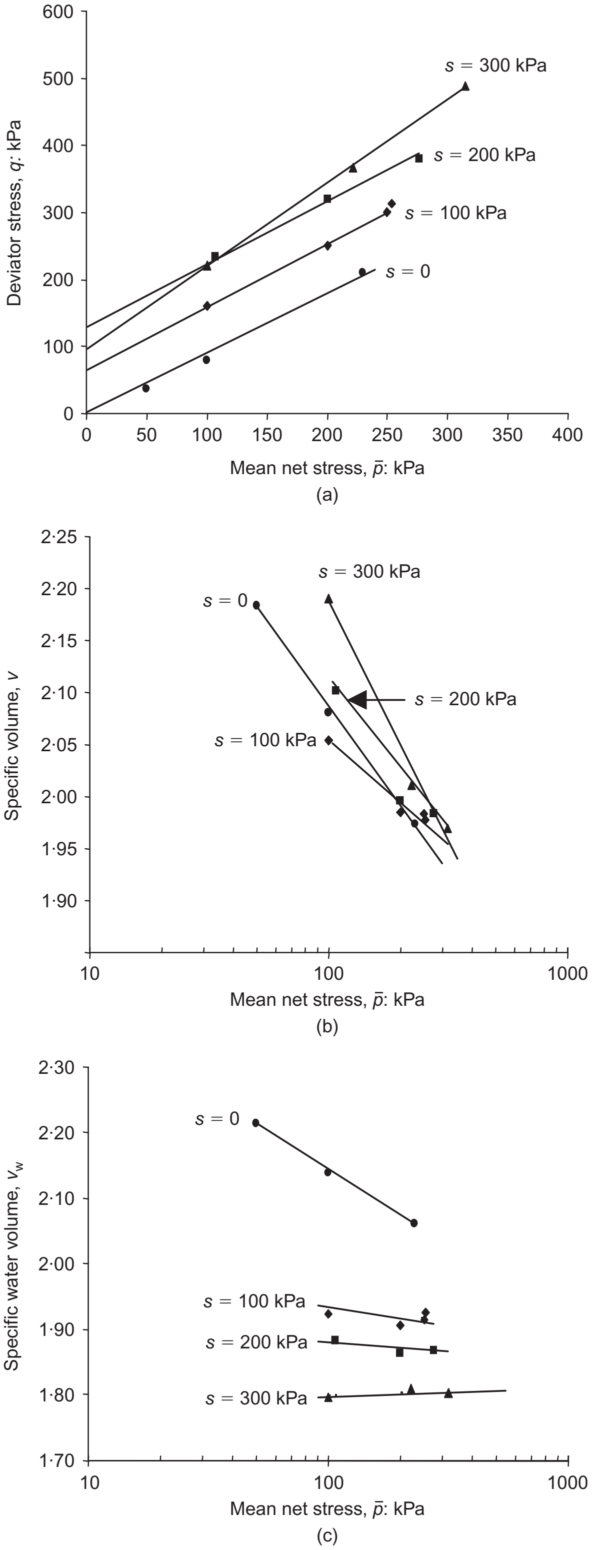

Fig. 4. Conditions at critical state for IS(A)

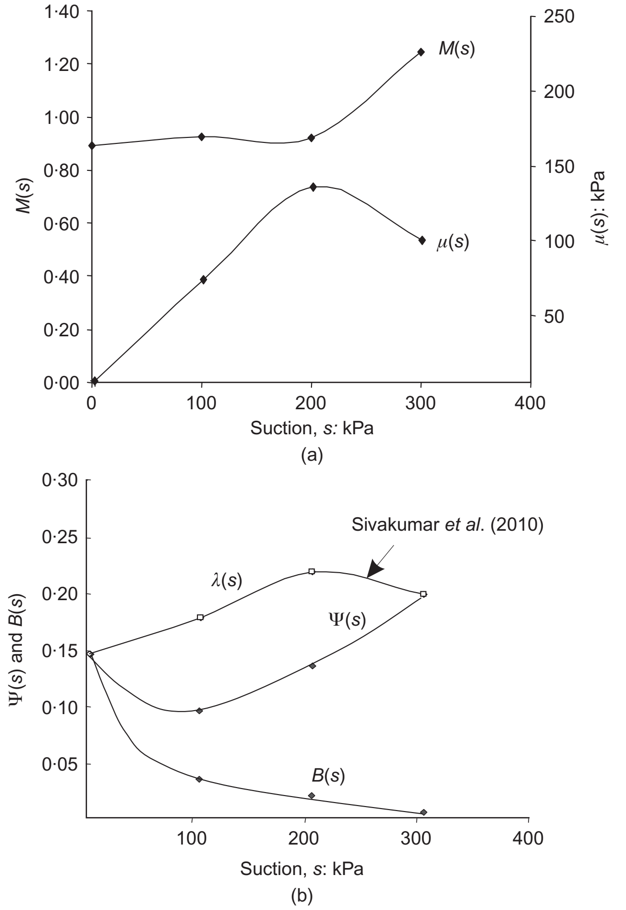

Fig. 5. Critical state parameters: (a) intercept and slope of critical state lines in terms of q: $\overline{p}$ plane; (b) slope of critical state lines in terms of v:ln($\overline{p}$)

Some early work on unsaturated soils had identified the variable effect of suction on the apparent cohesion induced by suction (Fredlund *et al.*, 1978; Escario & Saez, 1986). Fredlund *et al.* (1978) modified the Mohr–Coulomb criterion for the shear stress τ of saturated soils to accommodate unsaturated soils and proposed the following equation

$$\tau = c' + \overline{\sigma}_{\text{n}}\tan(\phi') + (u_{\text{a}} - u_{\text{w}})\tan\phi^{\text{b}} \tag{4}$$

where c' is the effective cohesion with a value of zero for normally consolidated soils. $\overline{\sigma}_{\text{n}}$, u_{a} and u_{w} are net normal stress, pore air pressure and pore water pressure respectively. ϕ' and ϕ^b are the angles of internal friction with respect to normal stress and suction respectively. Equations (4) and (1) describe similar conditions when the soil is normally consolidated. In particular, the last term in equation (4) is related to $\mu(s)$ in equation (1). Fredlund *et al.* (1978) have shown using experimental evidence that ϕ^b remains constant at low values of suction and decreases significantly at higher values of suction, a result which agrees with the findings from the present research. An argument for the reduction in the intercept, $\mu(s)$, with increasing suction, is that at high values of suction the water meniscus, which translates suction into useful inter-granular stresses, and thus resistance to shearing, is reduced (Gallipoli *et al.*, 2003; Wheeler *et al.*, 2003). The additional inter-granular stresses responsible for the enhancement of $\mu(s)$ are dependent on the degree of saturation within the inter-aggregate pore spaces. The accompanying paper postulated that the inter-aggregate voids were partly filled with water only at low values of suction ($s \approx 100$ kPa) and at elevated values of suction, when the water was drawn into the smaller intra-aggregate void spaces, the available water menisci between the aggregates were significantly reduced and unavailable to translate into additional cohesion.

As illustrated in Fig. 5(a), the slope of the critical state line, $M(s)$, significantly increases at a suction of 300 kPa. Escario & Saez (1986) presented experimental data generated using shear box apparatus under controlled suction, which highlighted a slight increase of the angle of internal friction, ϕ' (ϕ' in equation (4) is comparable with $M(s)$ in equation (1)) at high suction values. A possible reason for an increased angle of internal friction may lie in the way the aggregates respond during shear loading. The aggregates are generally saturated within the range of suctions considered in the present study. At high suction these saturated aggregates are subjected to very high effective stress (the term effective stress holds true only when the aggregates are saturated and evidence for this assertion is presented in the accompanying paper) as the effect of the suction is equivalent to an isotropic effective stress of the same magnitude (Doran *et al.*, 2000). It is plausible that the aggregates can thus be expected to exhibit a degree of rigidity with the interaction between them resembling that of a more granular material, hence resulting in a higher angle of internal friction.

Figure 4(b) shows the critical state lines in v: $\ln \overline{p}$ space for isotropically prepared samples at different values of suction. A linear relationship has been assumed for each suction value considered, consistent with equation (2). While the data intuitively support the existence of critical state conditions in v: $\ln \overline{p}$ space, the results indicate some inconsistency in relation to the positions of the critical state lines. For example, the critical state line at a suction value of 100 kPa is below that of zero, 200 kPa and 300 kPa of suction. Fig. 5(b) shows that the slopes of the critical state lines $\psi(s)$ from equation (2) are dependent on suction which agrees with Maãtouk *et al.* (1995), Wheeler & Sivakumar (1995, 2000) and Ng & Chiu (2001), but contradicts the conclusion of Wang *et al.* (2002), who suggested that the slope $\psi(s)$ is independent of suction and is equal to the slope of the saturated critical state line. According to constitutive modelling in saturated soils, the slope of the normal compression line $\lambda(s)$ is approximately equal to the slope of the critical state line. The slope $\lambda(s)$ is also included in Fig. 5(b). It is apparent that in the present study on unsaturated kaolin, the normal compression line is parallel to the critical state line only when the suction is reduced to zero or at a suction value of 300 kPa. The difference is significant at intermediate values of suction. Fig. 5(b) also shows the relationship between the slope of the critical state line in the v_w: $\ln \overline{p}$ plane and suction based on the results of Fig. 4(c). The slope $B(s)$ from equation (3) is equivalent to $\psi(s)$ (i.e., the slope of the critical state line in the v: $\ln \overline{p}$ (when suction is zero) and reduces significantly with increasing suction. There appears to be no drainage of water resulting from a change in mean net stress at a suction value of 300 kPa.

Yield surface in q: $\overline{p}$: s space for samples with isotropic stress history

Yielding is associated with the onset of plastic strain and is usually represented by a change in the stress–strain relationship (Graham *et al.*, 1988; Smith *et al.*, 1992; Navaneethan, 2003). The yielding of clay is controlled by both the deviator and mean effective stresses in saturated clays. In unsaturated soils, suction also has a significant effect. The yielding of clay at different stress ratios (i.e., $q/\overline{p}$ or q/s) forms a surface in q: $\overline{p}$: s space, which is examined here.

Yielding in the q: $\overline{p}$ plane. The determination of the yield stresses estimated from the plots of q against axial strain ε_a for samples of IS(A) at 300 kPa of suction is presented in Figs 6(a) and 6(b). The yield stress may also be estimated using the $v - \overline{p}$ relationship, an example of which is shown in Fig. 7 for fully drained shearing at a suction value of 300 kPa. The estimated values are in close agreement. Yield points estimated from the fully drained and constant mean

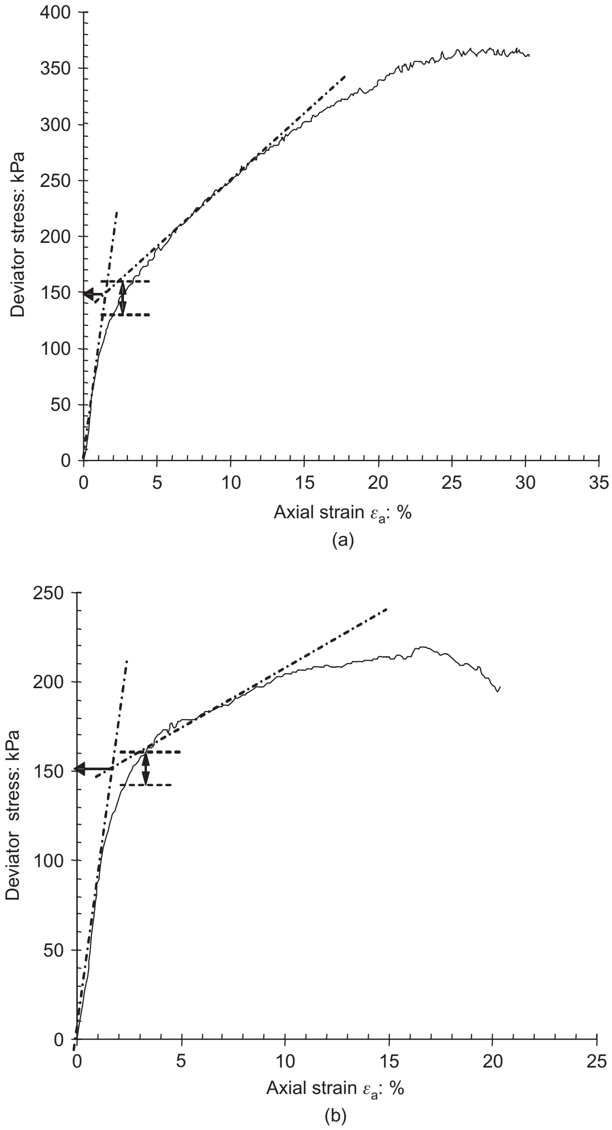

Fig. 6. Stress–strain curves of fully drained and constant mean net stress tests for IS(A): (a) fully drained; (b) constant mean net stress

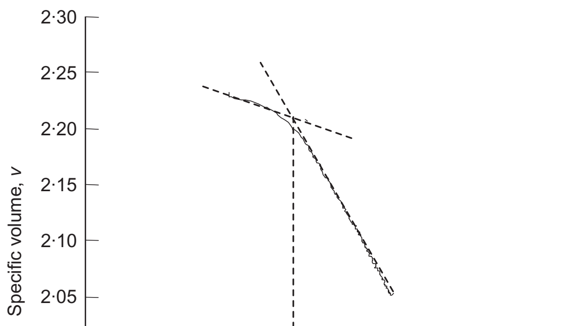

Fig. 7. Pressure–volume relationship (IS(A)); fully drained test at s = 300 kPa after normal compression to 100 kPa of mean net stress

net stress tests (tests 4B and 4A respectively in Table 1) are represented by points B and C in Fig. 8, which shows the yield locus in the q: $\overline{p}$ plane (constant s) for isotropically prepared samples. The additional point A was obtained from an isotropic compression test performed at a suction of 300 kPa (test 4d, Table 1 reported in the accompanying paper). The yield stresses marked on Fig. 8 are connected with a best fit elliptical curve. As can be seen, the ellipse is approximately symmetrical about the mean net stress axis. It also appears that the critical state line at a suction value of 300 kPa passes through point D at which $dq/d\overline{p}$ is approximately zero. This correlates with the classical proposal made in the modified Cam-Clay model for isotropic materials. It is probably coincidence that the intersection at point E of the ellipse on the negative $\overline{p}$ axis falls close to the intersection of the critical state line, if extended backwards.

Yielding in the q: s plane. Three tests on isotropically prepared samples, IS(A), were conducted to examine the yielding of unsaturated soils in the q:s plane (constant $\overline{p}$). As schematically illustrated in Fig. 9(a) the samples were initially allowed to equalize at a pre-selected suction value of 300 kPa under 50 kPa mean net stress to point C. The samples were then isotropically compressed to 100 kPa to point D, with suction maintained constant at 300 kPa. Stress path tests in the q:s plane were then conducted. One sample was sheared under the condition of $\Delta q/\Delta s = -0{\cdot}83$ representing reduction in suction, path DR (test 5A, Table 1). A further sample was sheared under the condition $\Delta q/\Delta s = 1{\cdot}66$ representing increasing suction, path DP. In these two tests the rate of change in suction was directly related to the change in deviator stress q which was determined by the sample itself. A third sample was tested at constant suction condition represented by path DQ. The mean net stress was maintained at 100 kPa in all the tests.

Figure 9(b) shows the stress–strain response of the specimens of IS(A) sheared under the different $\Delta q/\Delta s$ ratios. Note that the initial state of the samples was overconsolidated since the mean net stress of 100 kPa was well within the yield stress estimated from the isotropic compression test which showed a yield stress under isotropic loading of 210 kPa, as described in the accompanying paper. The initial behaviour of the soil can be described as reasonably elastic. The yield stresses estimated as shown in Fig. 9(b) are plotted in Fig. 10 to provide the yield curve in the q:s plane. A fourth point O

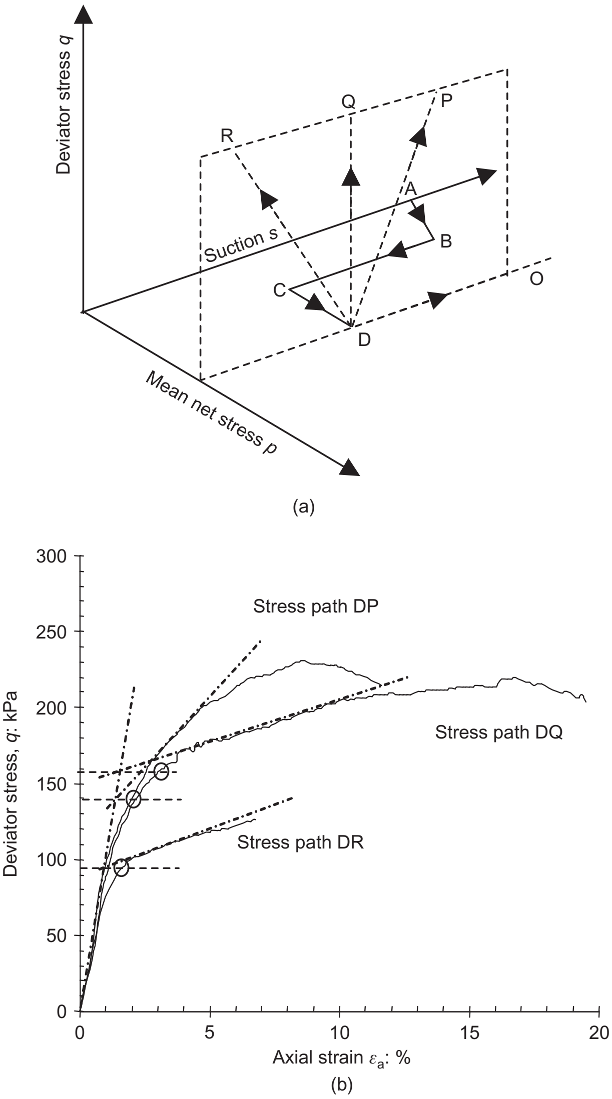

Fig. 9. Stress–strain curves at constant mean net stress of 100 kPa under varying suction for IS(A)

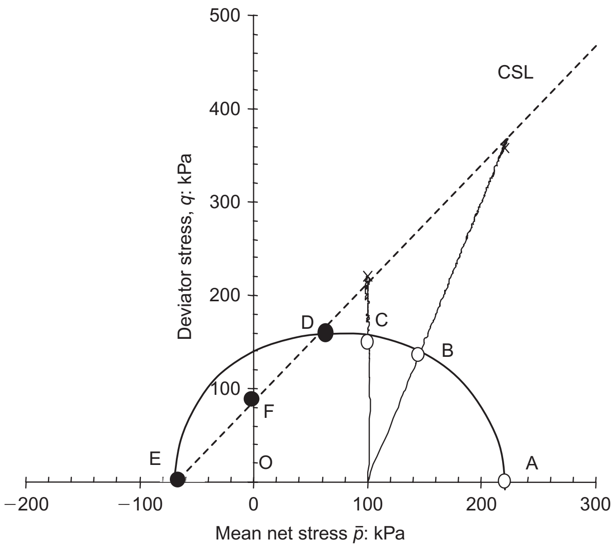

Fig. 8. Yield locus in the q: $\overline{p}$ plane at suction of 300 kPa for IS(A)

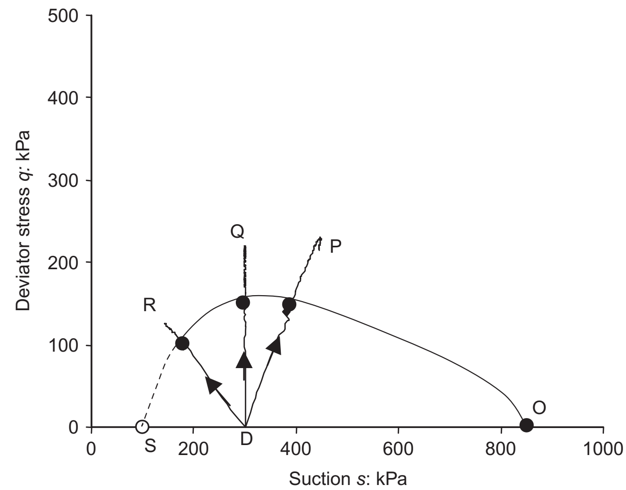

Fig. 10. Yield curve in the q:s plane for IS(A)

is shown in Fig. 10 at a suction of 850 kPa. This is the approximate maximum suction experienced by the sample in its formation and it can be expected that the sample would yield upon reapplication of suction (path DO in Fig. 9(a)). This assumption is based on the proposals of suction increase yield locus (SI) as proposed by Alonso *et al.* (1990). In the literature referring to unsaturated soil, limited experimental results have been reported for the yield envelope in the q:s plane. Alonso *et al.* (1990) argued that either increasing suction or deviator stress can produce yielding and plastic hardening. According to their model, if two tests are carried with one sample sheared under constant $\overline{p}$ and constant suction and the other sample sheared at constant $\overline{p}$ and increasing suction, then the yield deviator stress obtained from the latter should be larger. The experimental evidence obtained from the present research seems to differ from this model. The findings suggest that the shape of the yield envelope in q:s space is a curve of somewhat similar form to that postulated by Tang & Graham (2002). The yield locus intersects the s axis (direction of reducing suction) at point S (Fig. 10). This point also refers to the yield pressure that may emerge from a wetting test conducted at mean net stress of 100 kPa under zero deviator stress. This point can also be inferred from the LC yield locus for IS(A) presented in the companion paper (Fig. 12) and the yield suction at this point is approximately 105 kPa. The yield curves combined in $\overline{p}$: s: q space appear to produce a surface, with domed shape, although further research is necessary to corroborate the findings.

Effects of stress-induced anisotropy on the condition at critical state and yielding characteristics under controlled suction

The effects of anisotropy on the stress–strain behaviour of saturated soils are well established. Anisotropy, which can result from stress or deposition history, can significantly alter elastic and elasto-plastic behaviour. It is generally accepted that the yield locus is not symmetrical about the mean effective stress p' axis as in the case for isotropic material (Graham *et al.*, 1988) and research has shown that the major axis of the yield locus is approximately aligned along the K_0 line for saturated soils. Anisotropy also influences a soil's condition at critical state. The following discussion examines the relevance of the foregoing to the behaviour of unsaturated soils.

Figure 11 shows the critical state lines in q: $\overline{p}$ space

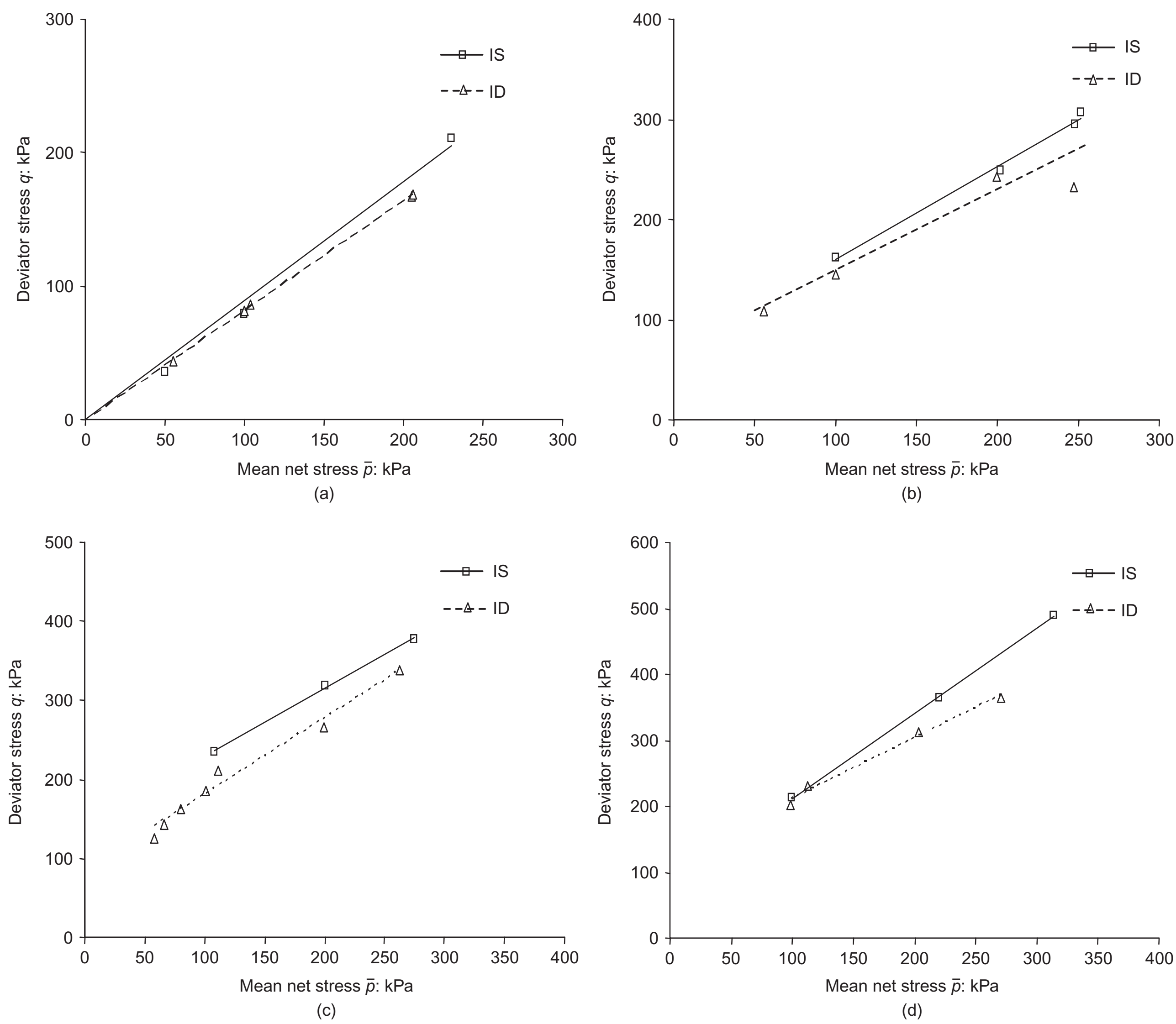

Fig. 11. Effects of stress-induced anisotropy at the critical state in the q: $\overline{p}$ plane: (a) $s = 0$; (b) $s = 100$ kPa; (c) $s = 200$ kPa; (d) $s = 300$ kPa

for samples prepared with suction values of zero, 100, 200 and 300 kPa. The square and triangular points represent, respectively, samples prepared using isotropic compression and one-dimensional compression. The relevant data are listed in Table 1 and Table 2 respectively. The critical state lines for isotropically compressed samples lie above the lines for one-dimensionally prepared samples in the q: $\overline{p}$ plane, implying that the strengths of isotropically compressed samples are greater. The differences are not large at zero suction but become more significant with increasing suction.

The slopes, $M(s)$, and the intercepts, $\mu(s)$, of the critical state lines are compared in Fig. 12. There is little difference in the values of $M(s)$ for isotropically and one-dimensionally compressed specimens for suctions up to 200 kPa. However, at 300 kPa of suction, the value of $M(s)$ for the isotropically compressed specimen is markedly greater than that for the one-dimensionally compressed sample. In contrast, values of $\mu(s)$ for isotropically compressed samples are greater than those of one-dimensionally compressed samples other than at a suction of 300 kPa, where the value of $\mu(s)$ is significantly less than that of the one-dimensionally compressed sample.

Figure 13 shows the critical state lines in v: $\ln(\overline{p})$ space for samples prepared using the two different procedures for suction values of zero, 100, 200 and 300 kPa. Also included are the positions of the normal compression lines for isotropically compressed and one-dimensionally compressed samples, traced by using the relevant slopes and intercepts of the normal compression lines reported in the companion paper. The normal compression lines (NCL) and critical state lines (CSL) for initially isotropically compressed samples lie above the corresponding lines for one-dimensionally compressed samples at all values of suction. Wheeler & Sivakumar (2000) reported a series of experimental data generated on one-dimensionally compressed samples prepared at two different initial densities. The work showed that although there appeared to be significant differences in the position of the normal compression lines, the positions of the critical state lines were generally unaffected by the initial specific volume of the samples at the time of preparation. The present research used isotropically compressed samples with an identical specific volume to those of the one-dimensionally compressed samples reported by Wheeler & Sivakumar (1995). It would appear that while the initial density of compression does not influence the critical state line, the method of compression (isotropic or one-dimensional) does.

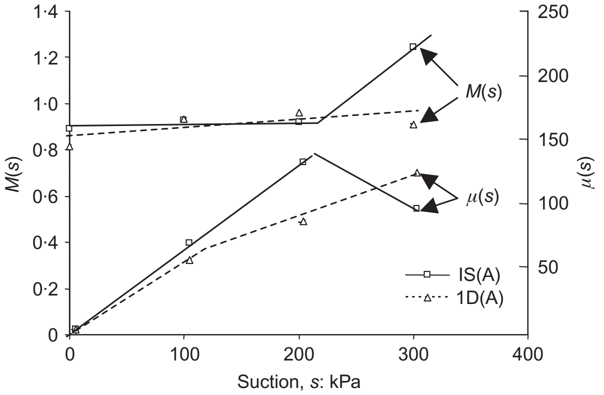

Fig. 12. Effects of stress-induced anisotropy on the critical state parameters

As noted for Fig. 11, the strength of isotropically compressed samples is higher than those of one-dimensionally compressed samples when plotted against the mean net stress for a given value of suction. Normally greater density of a material implies greater strength. However, the specific volumes of isotropically prepared samples at the critical state were significantly greater than those of one-dimensionally compressed samples. Fig. 14 shows the degree of saturation S_r plotted against $\overline{p}$ at the critical state for samples with isotropic and one-dimensional stress history. It appears that the sample with one-dimensional stress history ended with generally higher degrees of saturation at a given value of suction. While the results clearly indicate that the sample preparation technique influences the results, the control mechanism is not clear though it is possible to conjecture a number of

Table 2. Normally consolidated and critical state parameters (samples of ID(A))

Test no.	After isotropic compression				Critical state				
	$\overline{p}$: kPa	s: kPa	v	v_w	$\overline{p}$: kPa	s: kPa	q: kPa	v	v_w
1A (CV)	175	0	1·987	1·986	100	0	81	1·987	1·987
1B (CP)	55	0	2·115	2·114	55	0	43	2·086	2·086
1C (FD)	150	0	2·008	2·008	206	0	167	1·933	1·933
1D (FD)	150	0	2·005	2·004	206	0	168	1·938	1·938
1E (FD)	75	0	2·079	2·079	104	0	86	2·015	2·015
2A (CV)	150	100	2·042	1·840	56	100	108	2·042	1·879
2B (CP)	100	100	2·133	1·852	100	100	145	1·992	1·903
2C (CP)	200	100	1·998	1·845	200	100	242	1·909	1·872
2D (FD)	150	100	2·038	1·849	247	100	232	1·889	1·864
3A (CV)	100	200	2·162	1·781	59	200	126	2·162	1·808
3B (CV)	200	200	2·067	1·783	80	200	163	2·067	1·808
3C (CV)	150	200	2·127	1·784	67	200	143	2·127	1·815
3D (CV)	300	200	1·990	1·776	111	200	212	1·990	1·819
3E (CP)	100	200	2·172	1·771	101	200	186	2·033	1·823
3F (CP)	200	200	2·065	1·772	199	200	265	1·929	1·819
3G (FD)	150	200	2·099	1·779	263	200	338	1·875	1·811
3H (FD)	100	200	2·180	1·783	186	200	257	1·935	1·834
4A (CV)	250	300	2·053	1·725	113	300	232	2·053	1·757
4B (CP)	100	300	2·195	1·712	99	300	203	2·130	1·747
4C (FD)	100	300	2·188	1·726	203	300	313	1·945	1·775
4D (FD)	150	300	2·140	1·729	271	300	365	1·887	1·778

(CV), constant volume; (CP), constant mean net stress; (FD), fully drained

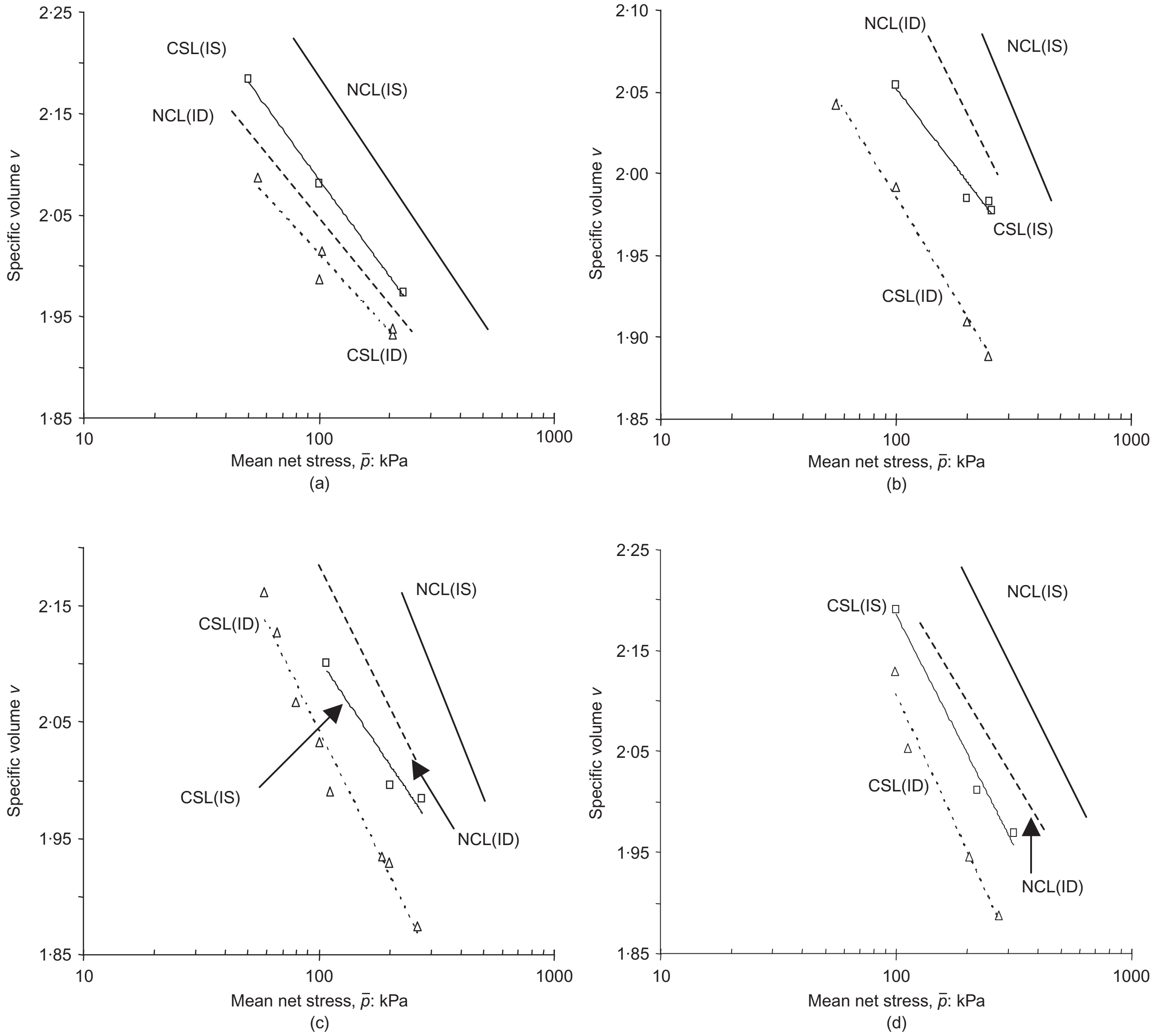

Fig. 13. Effects of stress-induced anisotropy at the critical state in the v: $\bar{p}$ plane: (a) $s=0$; (b) $s=100$ kPa; (c) $s=200$ kPa; (d) $s=300$ kPa

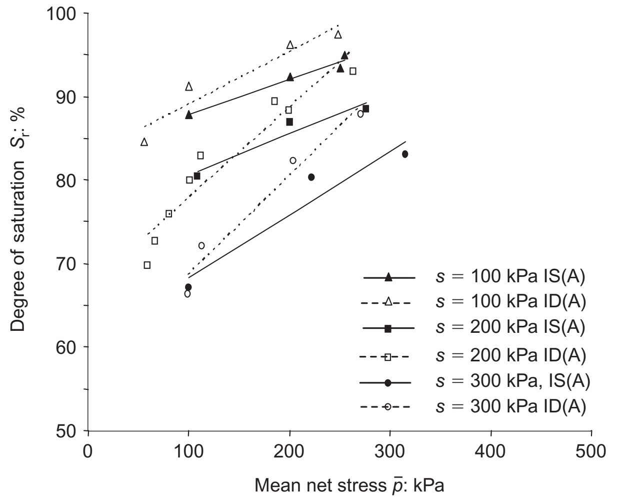

Fig. 14. Degree of saturation plotted against mean net stress at critical state

reasons for the observations, including the aggregate distribution, stiffness, breakage during shearing and fissuring as well as the influence of water-menisci between aggregates.

Figure 15 shows the stress–strain relationships obtained from isotropically compressed samples, IS(A), and one-dimensionally compressed samples, ID(A), which were subjected to fully drained loading (Fig. 15(a)) and constant $\bar{p}$ loading (Fig. 15(b)) at a suction of 300 kPa. Estimated yield stresses are plotted in Fig. 16 to form yield loci in the q: $\bar{p}$ plane for the different stress histories. The yield locus for isotropic stress history (shown by triangular data points) is that reproduced from Fig. 8. It is apparent that the samples of IS(A) exhibit an elliptical yield locus, which appears symmetrical about the $\bar{p}$ axis, and that for the ID(A) samples is rotated about the $\bar{p}$ axis. This is in good agreement with the discussion presented in the accompanying paper that the size of the LC yield locus of samples with a one-dimensional stress history was significantly smaller than that of samples with an isotropic stress history.

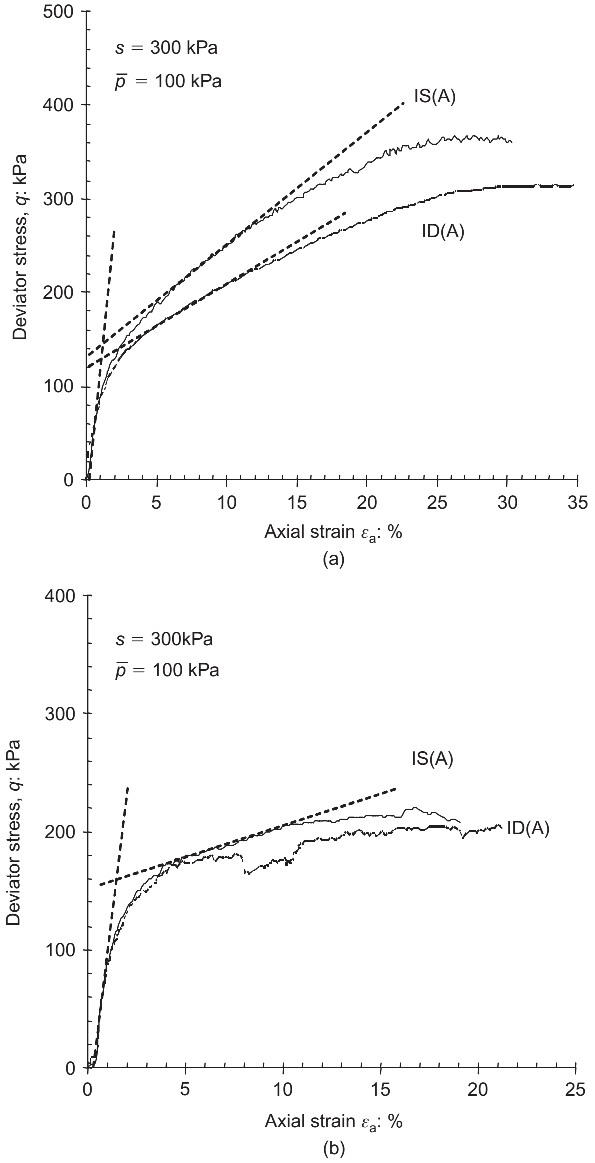

Fig. 15. Effects of stress-induced anisotropy on the stress–strain curve: (a) fully drained; (b) constant $\bar{p}$

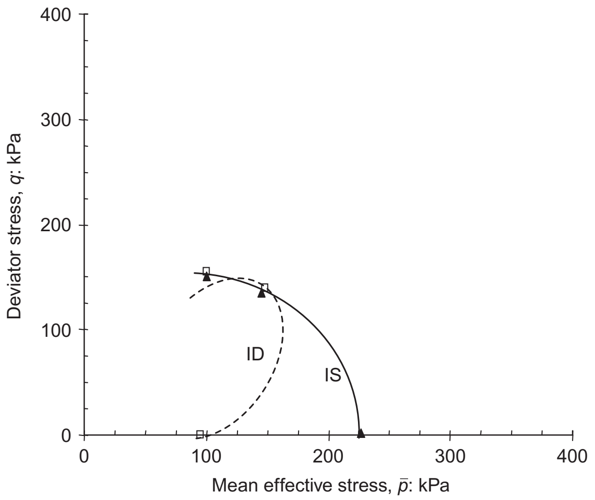

Fig. 16. Effects of stress-induced anisotropy on the yield locus of samples at suction of 300 kPa

Effects of stress-induced anisotropy on the stress–strain behaviour and stress paths of samples under constant water mass conditions

A number of unsaturated soil samples prepared using isotropic and one-dimensional compression, with identical initial specific volumes of 2·19 at water contents of 25%, were consolidated under designated isotropic stress conditions while water drainage valves were closed. When equilibrium was reached at the end of consolidation, the samples were sheared under constant water mass conditions (CWM) using the strain control method with the cell confining pressure maintained constant at the consolidation pressure.

Figure 17 shows the stress–strain responses of five CWM tests conducted on isotropically and one-dimensionally compressed samples under net confining pressures of 50 kPa, 100 kPa, 200 kPa, 300 kPa and 500 kPa. The initial and final conditions of the samples are listed in Table 3. The figure includes the variations of deviator stress, volumetric strain and suction plotted against axial strain. The deviator stress is shown to increase linearly up to around 1% axial strain and reaches a maximum value at an axial strain ranging from 15% to 30%. The samples sheared at higher confining pressure reached failure at a higher axial strain. There was no significant reduction in the deviator stress for samples tested at net confining pressure of 50 kPa and 100 kPa. However, the deviator stress for samples tested at net confining pressures of 200 kPa, 300 kPa and 500 kPa showed some post-peak reductions, implying that samples showed a brittle failure (strain-softening).

As shown in Fig. 17, the maximum value of the deviator stress increases with increasing confining stress. There appear to be no significant differences in the stress–strain curves between the two types of sample, although the samples with isotropic stress history exhibited higher values of deviator stress at failure. This observation is in good agreement with the findings from controlled suction tests (Fig. 11). Despite samples being prepared at identical water contents, isotropically compressed samples showed higher initial suction than those of one-dimensionally compressed samples at the beginning of the shearing process. All the samples (both isotropic and one-dimensionally compressed) showed a reduction in volume with shearing. The reduction in specific volume increased with increasing confining pressure. At low values of confining pressures, one-dimensionally compressed samples showed greater volume change than isotropically compressed samples, agreeing with the previous postulation that the aggregates were fissured and susceptible to breakdown, although those fissures may have closed up if the samples were compressed to high pressure before shearing.

Figure 17 also shows the variation of suction with axial strain during shearing under constant water mass conditions. The suction is shown to remain constant for isotropically compressed samples at all the confining pressures, suggesting no significant straining through individual aggregates during the shearing. However, the suctions for one-dimensionally compressed samples are shown to reduce with increasing axial strain implying that shear stresses generated an increase in pore water pressure. This observation contradicts the conclusion of Tang *et al.* (2002), from tests on bentonite-sand compacted one-dimensionally, that the variation of suction response was only attributable to the mean net stress and not affected by the deviator stress.

The responses of isotropically and one-dimensionally compressed samples during shear loading, shown in Fig. 18, are very interesting. The suction in one-dimensionally compressed samples reduced significantly during shear loading and the pattern was generally consistent among samples tested at various confining pressures. The initial part of the

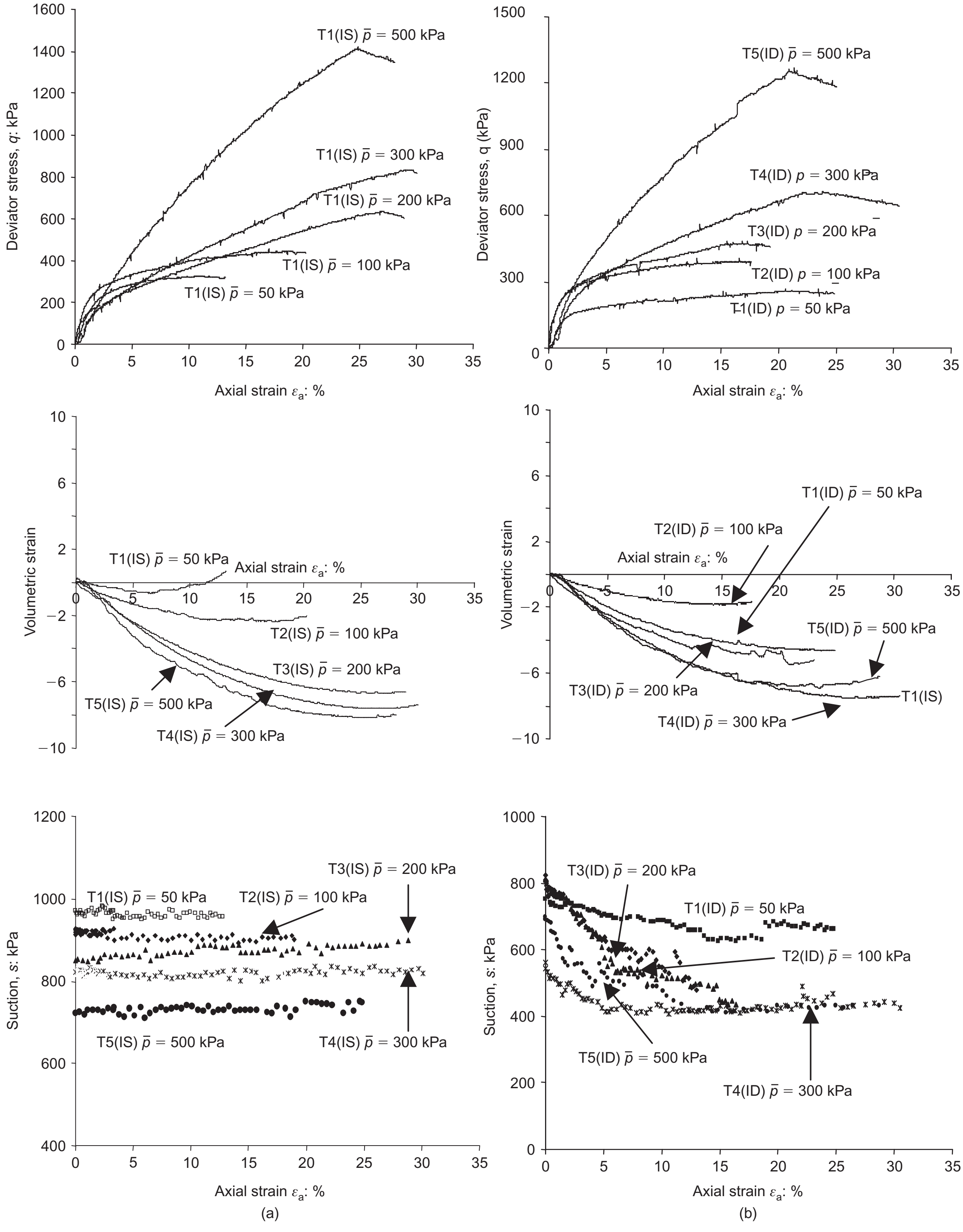

Fig. 17. Effects of stress-induced anisotropy on the stress–strain curves under constant water mass conditions: (a) isotropic previous stress history; (b) anisotropic previous stress history

stress path shown in Fig. 18 is generally linear with a slope $dq/ds = -0{\cdot}2$ and there appears to be a significant change in the responses at large strain. It is not clear whether it is a sign of yielding or the response of the sample to possible structural breakdown. However none of the above features seem to exist in the case of samples with isotropic history, also shown in Fig. 18, as the suction was unaffected by the deviator stress q.

The arguments in the previous section and the accompanying paper (Sivakumar *et al.*, 2010) have presented a case that, in the tests undertaken the individual aggregates were saturated and subjected to very high stresses as a result of the suction during sample formation. Other than at low values of suction, uptake of water by the soil samples was associated with uptake of water by the aggregates. The aggregates would have been overconsolidated (i.e., on an aggregate level) when the suction was reduced to low values in the controlled suction tests. In the constant water mass tests the suctions were not externally reduced from the initial values. It can be assumed that in these tests the individual aggregates were

Table 3. Conditions at failure (constant water mass tests)

Test no.	After isotropic compression				Critical state				
	$\overline{p}$: kPa	s: kPa	v	v_w	$\overline{p}$: kPa	s: kPa	q: kPa	v	v_w
Isotropically prepared samples (IS(A))									
1IS	50	973	2·185	1·647	153	970	325	2·183	1·647
2IS	100	930	2·191	1·653	241	931	440	2·133	1·653
3IS	200	851	2·167	1·662	406	888	633	2·005	1·662
4IS	300	808	2·156	1·658	575	811	833	1·992	1·659
5IS	500	745	1·989	1·655	917	750	1395	1·810	1·655
One dimensionally prepared samples (ID(A))									
1ID	50	747	2·195	1·669	140	679	265	2·090	1·669
2ID	100	824	2·127	1·647	229	495	395	2·096	1·647
3ID	200	812	2·155	1·650	366	445	482	2·058	1·650
4ID	300	560	2·119	1·660	533	452	714	1·981	1·660
5ID	500	690	2·017	1·664	909	430	1231	1·885	1·664

normally (i.e., on an aggregate level) or only slightly overconsolidated. Analogous with normally consolidated saturated soils, shear straining of aggregates in the CWM tests can thus be expected to result in a reduction in suction (increase in pore water pressure). However, the initially one-dimensionally prepared samples of Fig. 18 show a reduction in suction, but the isotropically prepared samples do not. The only possible reason for this difference is that the aggregates of the isotropically compressed samples experienced less significant shear straining during the shear loading, possibly because less fissuring developed at the time of sampling.

Figure 19 also shows a distinct difference in the shear behaviour of isotropically and one-dimensionally prepared samples, obtained through controlled suction tests. The figure shows the change in specific water volume plotted against axial strain for samples subject to fully drained constant suction tests at 100, 200 and 300 kPa of suction. Since the specific water volume represents approximately the volume of the saturated aggregates per unit volume of solids, a change in specific water volume represents a change in the volume of the aggregates. Positive specific water volume change represents an increase in water content. In the case of low values of suction it is apparent that water intake by one-dimensionally compressed samples is significantly greater implying that the soil, and in particular the aggregates, achieved the point of strain softening well ahead of isotropically compressed samples, on the assumption that the aggregates were overconsolidated prior to shearing.

Figure 20 shows the stress paths of CWM tests performed on three samples prepared using one-dimensional compression. Samples 1 and 2 were initially wetted to suction values of 100 kPa and 200 kPa prior to shearing under CWM conditions at a mean net stress of 100 kPa. In the case of sample 3, the CWM loading began without reducing the suction from its initial value. The observed behaviour possibly supports the fact that aggregates were normally or lightly overconsolidated at high values of suction (where the suction was not reduced prior to shearing) and were heavily overconsolidated at low values of suction (where suction was reduced to lower values prior to shearing), represented by a slight reduction and subsequent increase in suction values during shear loading.

CONCLUSIONS

This paper describes a detailed testing programme and the analysis carried out on samples of unsaturated kaolin with inherited isotropic and anisotropic (one-dimensionally compressed) properties. The testing was carried out to assess the effects of sample preparation on the conditions at critical state, the stress–strain behaviour during shearing, and the yield characteristics. The samples were sheared to critical state by various stress paths while either suctions or water masses were held constant. The results have been analysed adopting the simple linear equations proposed by Wheeler & Sivakumar (1995).

Critical state conditions represented by constant volume and stress conditions were shown to exist for both types of sample preparation, regardless of the direction of the stress path adopted under compression loading. However the effects of stress-induced anisotropy during sample preparation had a significant effect on the actual position of the critical state line, suggesting that the structure is not necessarily completely destroyed, to some extent deviating from the concept of critical state conditions as applied to saturated soils.

The shear strength of samples with inherited isotropic stress history was notably greater than that of one-dimensionally compressed samples when plotted against the mean net stress. The normal and critical state compression lines for isotropically prepared samples also appeared above the corresponding lines for one-dimensionally prepared samples when plotted against the mean net stress.

The yield locus of isotropically compressed samples is shown to correspond closely to an ellipse with the major axis coincident with the axis of mean net stress, whereas there is evidence to suggest that the yield locus of one-dimensionally compressed samples is approximately oriented along the K_0 line.

The results obtained from CWM tests agreed with the main findings from controlled suction tests at suction values up to 300 kPa. The suctions in CWM tests on one-dimensionally compressed samples were significantly affected by the deviator stress but the isotropically prepared samples showed little or no suction change under shearing.

ACKNOWLEDGEMENTS

The authors would like to thank Dr Gabriel Gallagher (Glover Site Investigation Limited, Northern Ireland), K. V. Senthilkumaran and P. J. Carey (P. J. Careys Contractors, UK) and J. Vimalan (VJ Tech Ltd, Reading, UK) for unconditional financial contributions to support geotechnical research at Queen’s University Belfast.

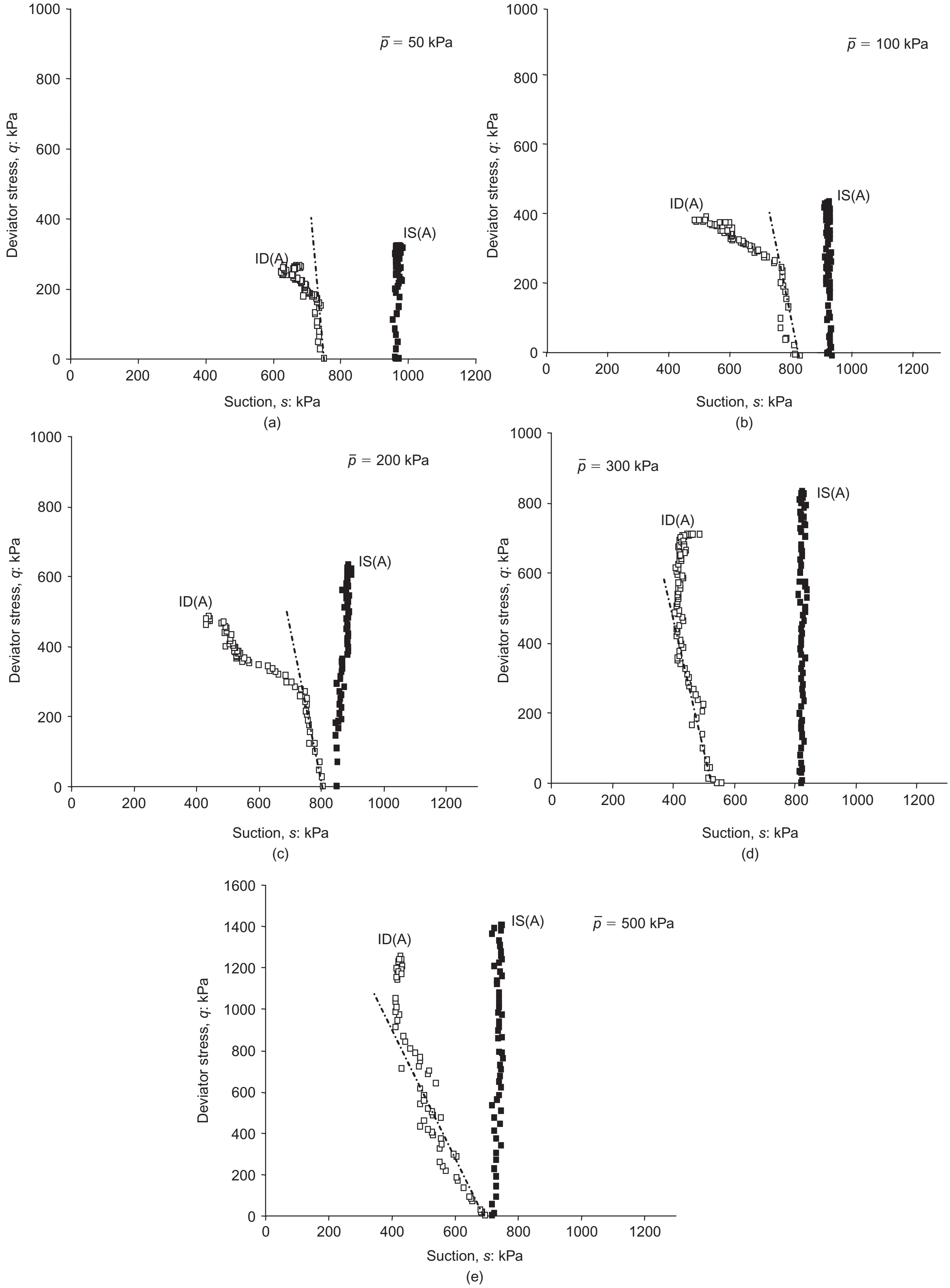

Fig. 18. Effects of stress-induced anisotropy on the stress path under constant water mass conditions.

NOTATION

$A(s)$ slope of v_w–ln($\bar{p}$) plot
$B(s)$ intercept of v_w–ln($\bar{p}$) plot
c' effective cohesion
K_0 coefficient of earth pressure at rest
p' mean effective stress
$\bar{p}$ mean net stress
$p_{\text{–atm}}$ atmospheric pressure
q deviator stress
s suction
u_a pore air pressure
u_w pore water pressure
v volume
v_w specific water volume
$\Gamma(s)$ intercept of critical state line in v–ln($\bar{p}/p_{\text{–atm}}$) plot
$\mu(s)$ intercept of critical state line in q: $\bar{p}$ plot

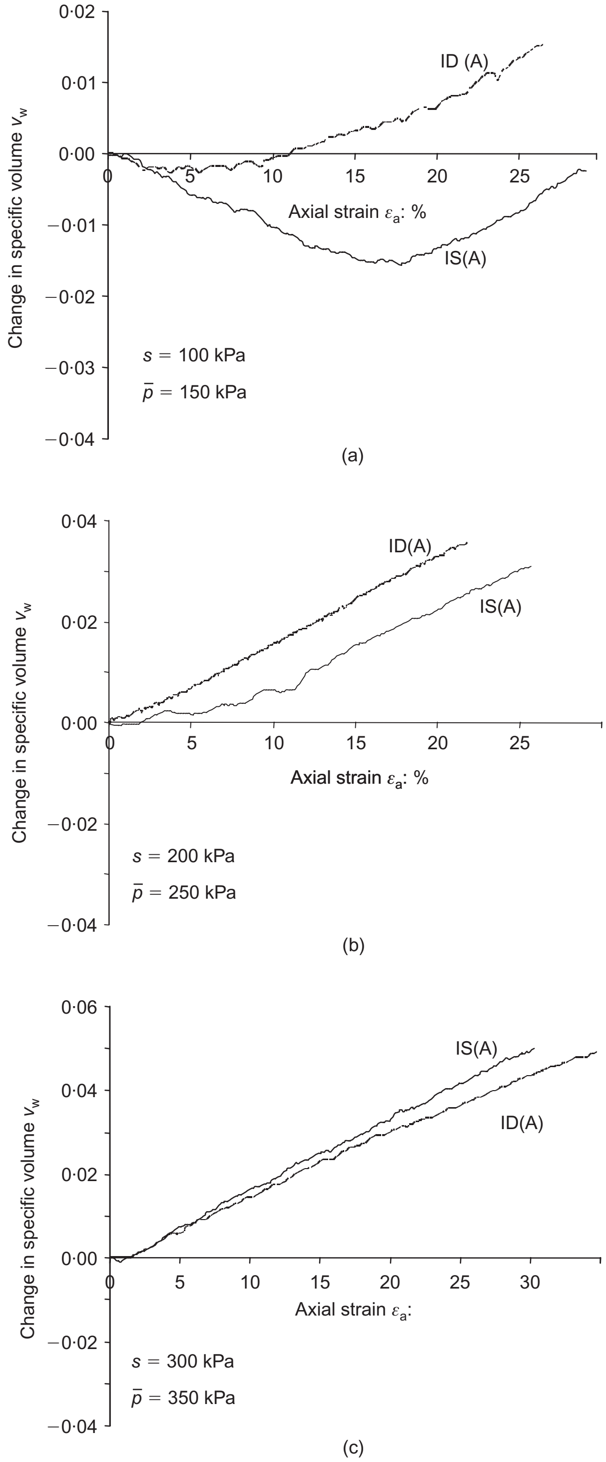

Fig. 19. Effects of stress-induced anisotropy on the water volume change during shearing

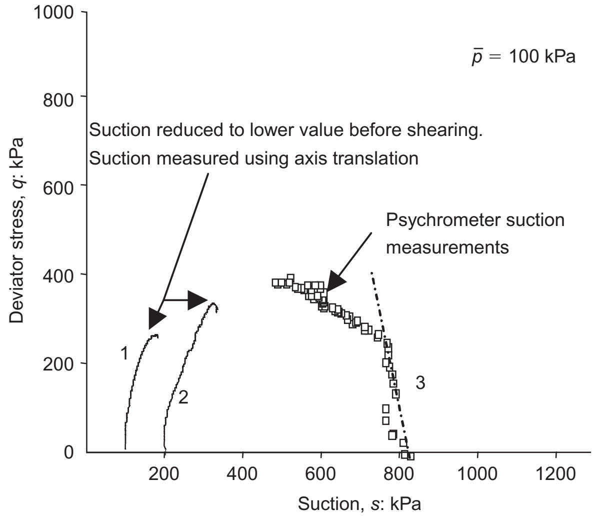

Fig. 20. Suction changes during constant water mass loading (ID(A))

$M(s)$ slope of critical state line in q: $\bar{p}$ plot
ϕ' angle of internal friction with respect to normal stress
ϕ^b angle of internal friction with respect to suction
σ_n normal stress
$\psi(s)$ slope of critical state line in v–ln($\bar{p}/p_{-\text{atm}}$) plot
τ shear stress

REFERENCES

Alonso, E. E., Gens, A. & Hight, D. W. (1987). Special problem soils: General Report. *Proc. 9th Eur. Conf. Soil Mech., Dublin*, **3**, 1087–1146.

Alonso, E. E., Gens, A. & Josa, A. (1990). A constitutive model for partially saturated soils. *Géotechnique* **40**, No. 3, 405–430.

Bishop, A. W. & Blight, E. (1963). Some aspects of effective stress in saturated and partially saturated soils. *Geotechnique* **13**, No. 3, 177–197.

Blatz, J. A. & Graham, J. (2003). Elastic–plastic modelling of unsaturated soil using results from a new triaxial test with controlled suction. *Géotechnique* **53**, No. 1, 113–122.

Chiu, C. F. & Ng, C. W. W. (2003). A state-dependent elasto-plastic model for saturated and unsaturated soils. *Géotechnique* **53**, No. 9, 809–829.

Cui, Y. J. & Delage, P. (1996). Yielding and plastic behaviour of an unsaturated compacted silt. *Géotechnique* **46**, No. 2, 291–311.

Doran, I. G., Sivakumar, V., Graham, J. & Johnson, A. (2000). Estimation of *in-situ* stresses using anisotropic elasticity and suction measurements. *Geotechnique* **50**, No. 2, 189–196.

Escario, V. & Saez, J. (1986). The shear strength of partly saturated soils. *Géotechnique* **36**, No. 3, 453–456.

Fredlund, D. G., Morgenstern, N. R. & Widger, R. G. (1978). The shear strength of unsaturated soils. *Can. Geotech. J.* **16**, 313–321.

Futai, M. M. & Almeida, M. S. S. (2005). An experimental investigation of the mechanical behaviour of an unsaturated gneiss residual soil. *Géotechnique* **55**, No. 3, 201–213.

Gallipoli, D., Gens, A., Sharma, R. & Vaunat, J. (2003). An elasto-plastic model for unsaturated soil incorporating the effects of suction and degree of saturation on mechanical behaviour. *Géotechnique* **53**, No. 1, 123–135.

Graham, J. & Houlsby, G. T. (1983). Anisotropic elasticity of a natural clay. *Géotechnique* **33**, No. 2, 165–180.

Graham, J., Crooks, H. A. & Lau, S. L. K. (1988). Yield envelopes: identification and geometric properties. *Géotechnique* **38**, No. 1, 125–134.

Leroueil, S., Kabbaj, M., Tavenas, F. & Bouchard, R. (1985). Stress–strain–strain rate relation for the compressibility of sensitive natural clays. *Géotechnique* **35**, No. 2, 159–180.

Leroueil, S. & Vaughan, P. R. (1990). The general and congruent effects of structure in natural soils and weak rocks. *Geotechnique* **40**, No. 3, 467–488.

Lings, M. L., Pennington, D. S. & Nash, D. F. T. (2000). Anisotropic stiffness parameters and their measurement in a stiff natural clay. *Géotechnique* **50**, No. 2, 109–125.

Maâtouk, A., Leroueil, S. & La Rochelle, P. (1995). Yielding and critical state of a collapsible unsaturated silty soil. *Géotechnique* **45**, No. 3, 465–477.

Navaneethan, T. (2003). *Pre-yield characteristics and earth pressure coefficient of overconsolidated clays*. PhD thesis. Queen's University Belfast, UK.

Ng, C. W. W. & Chiu, A. C. F. (2001). Behaviour of a loosely compacted unsaturated volcanic soil. *J. Geotech. Geoenviron. Engng* **127**, No. 12, 1027–1036.

Sivakumar, V., Sivakumar, R., Murray, E. J., Mackinnon, P. & Boyd,

J. (2010). Mechanical behaviour of unsaturated kaolin (with isotropic and anisotropic stress history). Part 1: wetting and compression behaviour. *Géotechnique* doi: 10.1680/geot.8.P.007.

Sivakumar, V. & Wheeler, S. J. (2000). Influence of compaction procedure on the mechanical behaviour of an unsaturated compacted clay. Part 1: wetting and isotropic compression. *Géotechnique* **50**, No. 4, 359–368.

Smith, P. R., Jardine, R. T. & Hight, D. W. (1992). The yielding of Bothkennar clay. *Géotechnique* **42**, No. 2, 265–274.

Tang, G. X., Graham, J., Blatz, J., Gray, M. & Rajapakse, R. K. N. D. (2002). Suction, stresses and strengths in unsaturated sand-bentonite. *Engng Geol.* **64**, No. 4, 147–156.

Tang, G. X. & Graham, J. (2002). A possible elastic–plastic framework for unsaturated soils with high-plasticity. *Can. Geotech. J.* **38**, 894–907.

Toll, D. G. (1990). A framework for unsaturated soil behaviour. *Géotechnique* **40**, No. 1, 31–44.

Wang, Q., Pufahl, D. E. & Fredlund, D. G. (2002). A study of critical state on an unsaturated silty soil. *Can. Geotech. J.* **39**, No. 1, 213–218.

Wheeler, S. J. & Sivakumar, V. (1995). An elasto-plastic critical state framework for unsaturated soil. *Géotechnique* **45**, No. 1, 35–53.

Wheeler, S. J. & Sivakumar, V. (2000). Influence of compaction procedure on the mechanical behaviour of an unsaturated compacted clay. Part 2: shearing and constitutive modelling. *Géotechnique* **50**, No. 4, 369–376.

Wheeler, S. J., Sharma, R. S. & Buisson, M. S. R. (2003). Coupling of hydraulic hysteresis and stress–strain behaviour in unsaturated soils. *Géotechnique* **53**, No. 1, 41–54.